ChemComm

ROYAL SOCIETY OF CHEMISTRY

COMMUNICATION

View Article Online
View Journal | View Issue

Cite this: *Chem. Commun.*, 2023, 59, 6371

Received 6th March 2023,
Accepted 1st May 2023

DOI: 10.1039/d3cc01115a

rsc.li/chemcomm

$CaFeFeNbO_6$ – an iron-based double double perovskite†‡

K. Ji,[a] J. R. Bedward,[a] Q. Li,[a] P. Manuel,[b] C. Ritter[c] and J. Paul Attfield*[a]

Ordering of cations is important for controlling properties of ABO_3 perovskites, and $CaFeFeNbO_6$ is the first example of an Fe-based $AA'BB'O_6$ double double perovskite, with Ca^{2+}/Fe^{2+} ordered on A-site columns, and Fe^{3+}/Nb^{5+} at the octahedral B-sites. Substantial (37%) antisite disorder of the latter cations leads to spin glassy magnetism below a freezing transition at 12 K. The $CaMnFeNbO_6$ analogue also shows substantial cation disorder and spin glassy behaviour. Comparison of synthesis pressures for ordered materials based on different A-site transition metals, suggests that pressures of at least 14–18 GPa will be required to discover the expected plethora of double double perovskites based on A' cations smaller than Mn^{2+}.

Cation ordering within ABO_3 perovskite oxides generates new structures and emergent physical properties,[1] most famously in B-cation ordered $A_2BB'O_6$ double perovskites where rock-salt ordering of B/B' transition metal cations[2–4] leads to ferrimagnetism and large magnetoresistance in Sr_2FeMoO_6 and related materials.[5,6] A variety of $AA'B_2O_6$ double perovskites based on columnar A-cation ordering has also been discovered through high pressure synthesis. This was first reported in $CaFeTi_2O_6$, synthesised at 12–15 GPa,[7] and several series based on A-site ordering of rare-earth (R) and Mn cations with the same $P4_2/nmc$ double perovskite structure; *e.g.* $RMn(Ga_{0.5}Ti_{0.5})_2O_6$ and $RMn(Mn,Ti)_2O_6$, have subsequently been reported from syntheses at lower pressure (6 GPa).[8–11] $CaMnTi_2O_6$ and $CaMn(Ti,V)_2O_6$ derivatives have a symmetry-lowered $P4_2mc$ double perovskite structure where loss of an inversion centre gives rise to ferroelectricity.[12,13] Combining the columnar A-site order with 1 : 1 order of B-cations gives rise to $AA'BB'O_6$ double double perovskites. RMn_3O_6 ($NaNbO_3$-type, *Pmmn*) materials have columnar R/Mn A-site and layered Mn charge-ordering at the B-sites,[14] but double perovskites based on orders of different metals have a tetragonal $P4_2/n$ structure with columnar A/A' and rocksalt type B/B' orders.

Many $P4_2/n$ $AA'BB'O_6$ double double perovskites with A' = Mn have been synthesised at 10 GPa; $RMnMnB'O_6$ (B' = Sb[15,16] and Ta[17]) and $CaMnBB'O_6$ (B = Mn, Fe, Co, Ni for B' = Re,[18–20] and B/B' = Fe/Ta,[21] Cr/Sb, Fe/Sb[22] and Mn/W[23]); and recently the first non-Mn analogue $CaCuFeReO_6$ was made at 15.5 GPa.[24] The $CaA'FeReO_6$ (A' = Mn, $Mn_{0.5}Cu_{0.5}$, Cu) materials are notable as ferrimagnets with Curie temperatures above 500 K and varying magnetoresistance properties.[18,24] Recovery of $CaCuFeReO_6$ from 15.5 GPa suggests that many further $AA'BB'O_6$ double double perovskites based on other A' metals may be accessible at pressures above 10 GPa. A' = Fe is a likely possibility given the columnar cation ordering in double perovskite $CaFeTi_2O_6$. A-site Fe^{2+} perovskites are of interest given the predominance of (Mg, Fe)SiO_3 perovskite in earth's lower mantle, and may have notable magnetic properties such as the unusual multiple-sublattice Fe^{2+} spin order recently reported in $CaFe_3Ti_4O_{12}$,[25] which has $1Ca^{2+}:3Fe^{2+}$ A-site order, but such recovered materials are rare. We report here high pressure exploration of $CaFeFeNbO_6$ and the Mn-comparator $CaMnFeNbO_6$, leading to the discovery that both form $P4_2/n$ double double perovskites although with significant B-cation disorder leading to spin-glass ground states.

Samples of ideal composition $CaMFeNbO_6$ (M = Mn, Fe) were treated under high pressure and high temperature conditions in a Walker-type multianvil press. The precursor mixture comprised stoichiometric amounts of $Ca_2Fe_2O_5$ (obtained by heating a pellet of $CaCO_3$ and Fe_2O_3 at 1200 °C for 24 h under an N_2 flow), MO (M = Mn, Fe) and Nb_2O_5. The mixture was packed into a Pt capsule, compressed to the synthesis pressure, heated over 10 minutes to the synthesis temperature, held at this temperature for 30 minutes, quenched to room temperature, and decompressed to ambient pressure. For M = Mn,

[a] *Centre for Science at Extreme Conditions (CSEC) and School of Chemistry, The University of Edinburgh, EH9 3FD, UK. E-mail: j.p.attfield@ed.ac.uk*
[b] *STFC Rutherford Appleton Lab, ISIS Facility, Harwell Science and Innovation Campus, Didcot, OX11 0QX, UK*
[c] *Institut Laue-Langevin, 38042 Grenoble Cedex, France*

† Data that support the findings of this study have been deposited at https://datashare.is.ed.ac.uk/handle/10283/838.

‡ Electronic supplementary information (ESI) available: Supporting figures and tables. See DOI: https://doi.org/10.1039/d3cc01115a

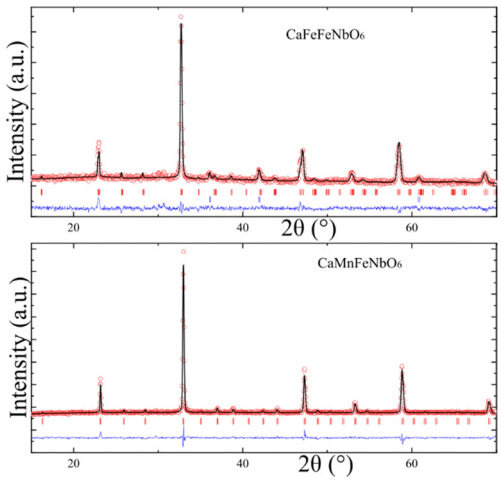

Fig. 1 Rietveld fits to room temperature PXD patterns of $CaMFeNbO_6$ (M = Mn, Fe) samples. A $P4_2/n$ double double perovskite model is fitted in both cases, although PXD does not discriminate well between possible superstructures. Lower Bragg markers for M = Fe are for FeO impurity.

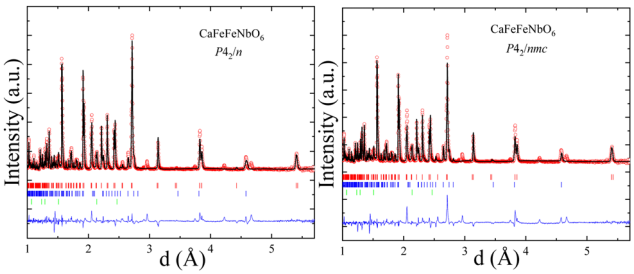

Fig. 2 Comparison of Rietveld fits to PND data for $CaFeFeNbO_6$ collected at 300 K using (left) the $P4_2/n$ double double perovskite (residuals: R_p = 4.91%, R_{wp} = 7.22%, R_{Bragg} = 6.28%, R_F = 3.23%), and (right) a $P4_2/nmc$ double perovskite model (R_p = 7.16%, R_{wp} = 10.30%, R_{Bragg} = 14.30%, R_F = 8.37%). Secondary phase markers are for $CaFeO_{3-x}$ (16.2(1)%) and FeO (8.2(1)%) and small unidentified impurity peaks are also observed in the difference curve.

reactions were performed at 10–12 GPa and 1000–1200 °C, and the optimum synthesis conditions were found to be 10 GPa and 1200 °C. Reactions were performed at 10–14 GPa and 1000–1400 °C for M = Fe, and the optimum synthesis conditions were found to be 14 GPa and 1400 °C. Laboratory powder X-ray diffraction (PXD) patterns were collected using a D2 Bruker diffractometer and powder neutron diffraction (PND) data were measured at the WISH beamline of the ISIS facility,[26] and on diffractometer D20 at ILL. Magnetization was measured using an MPMS SQUID magnetometer.

Powder X-ray diffraction showed that both $CaMFeNbO_6$ (M = Mn, Fe) compositions form a majority perovskite-structured phase at the optimum conditions above. However, secondary phases were present and were not eliminated in repeated syntheses. Fits to the PXD data (Fig. 1) demonstrate that both products are consistent with the $P4_2/n$ double double perovskite structure, although X-ray scattering does not discriminate well between different superstructure models and PND refinements were used to resolve these issues. Further results for $CaMnFeNbO_6$ are shown in ESI‡ Fig. S1–S7.

Fits to high resolution time-of-flight PND data for the $CaFeFeNbO_6$ sample show that the main phase is a cation-ordered perovskite, but $CaFeO_{3-x}$ perovskite, FeO and unidentified impurity are also observed. A-cation occupancies were varied in initial refinements but no disorder or off-stoichiometry was found, in keeping with the very different respective coordination numbers of 10 and 4 at Ca and Fe sites. The PND data do not show a clear superstructure peak from Fe/Nb B-site ordering (expected at d = 4.4 Å), so refinements of $P4_2/nmc$ double perovskite ($CaFe(Fe_{0.5}Nb_{0.5})_2O_6$ where B-cations are fully disordered) and $P4_2/n$ double double perovskite ($CaFeFeNbO_6$ with partial or full Fe/Nb order) models were compared, making use of the good Fe/Nb neutron contrast (b = 9.54/7.05 fm), as shown in Fig. 2. Comparison of the fits by eye and through their residuals shows that the double double perovskite model gives a substantially better fit, so this is taken to be the best structural description. Refinement results are shown in Table 1 and Fig. 3.

$CaFeFeNbO_6$ is confirmed as having the $P4_2/n$ double double perovskite structure, and so is the first reported Fe-based material in this family. Results in Table 1 show a substantial (37%) Fe/Nb antisite disorder at the B-sites. A similar (34%) antisite disorder was reported in the double perovskite Ca_2FeNbO_6,[27] and no long range Fe/Nb cation order was found in a recent neutron diffraction study of Sr_2FeNbO_6.[28] Disorder between Fe^{3+} and Nb^{5+} accounts for the lack of a clear superstructure peak at d = 4.4 Å for $CaFeFeNbO_6$, and likely reflects their similar ionic radii (0.645 and 0.64 Å respectively) and a formal charge difference of only 2. Synthesis at higher pressure or lower temperature might reduce the disorder. Despite their similar radii, the average B1–O = 1.97 Å distance for the Nb-rich site is smaller than B2–O = 2.05 Å for the Fe-rich site. This may reflect disordered off-centre second-order Jahn–Teller distortions for d^0 Nb^{5+} that reduce the crystallographic average

Table 1 Crystal structure parameters for $CaFeFeNbO_6$ from the 300 K $P4_2/n$ neutron Rietveld fit with derived bond distances (Å) below. Cell parameters are a = 7.6485(1) and c = 7.7145(2) Å. Residuals are shown in the Fig. 2 caption

Atom, Wyckoff site	x	y	z	B_{iso} (Å^2)	Occ
Ca, 4e	0.2500	0.7500	0.7791(1)	1.5(2)	1
A1(Fe), 2a	0.7500	0.7500	0.7500	1.6(1)	1
A2(Fe), 2b	0.2500	0.2500	0.7500	1.6	1
B1(Fe/Nb), 4c	0.0000	0.5000	0.5000	1.6	0.37(3)/0.63
B2(Fe/Nb), 4d	0.0000	0.0000	0.5000	1.6	0.63/0.37
O1, 8g	−0.065(1)	0.548(1)	0.243(1)	1.4(1)	1
O2, 8g	−0.248(2)	−0.043(1)	0.575(1)	1.4	1
O3, 8g	−0.227(1)	0.059(1)	−0.039(1)	1.4	1

Ca–O1(x2)	2.685(8)	B1–O1(x2)	2.08(1)
Ca–O1(x2)	2.877(6)	B1–O2(x2)	2.03(1)
Ca–O2(x2)	2.508(6)	B1–O3(x2)	1.82(1)
Ca–O3(x2)	2.486(8)	<B1–O>	1.97(1)
Ca–O3(x2)	2.359(8)	B2–O1(x2)	1.97(1)
<Ca–O>	2.583(8)	B2–O2(x2)	2.02(1)
A1–O2(x4)	2.084(5)	B2–O3(x2)	2.17(1)
A2–O1(x4)	2.104(8)	<B2–O>	2.05(3)

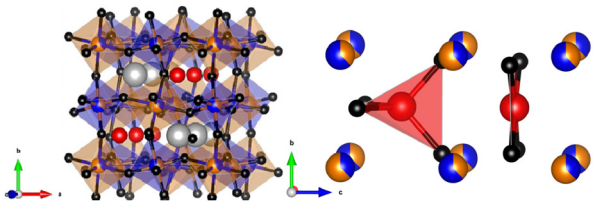

Fig. 3 Crystal structure of the tetragonal $P4_2/n$ AA′BB′O_6 double double perovskite $CaFeFeNbO_6$. A/A′/B/B′ sites are grey/red/blue/brown and Fe/Nb disorder is shown within the B/B′ octahedra. Detail at the right shows alternating square planar and tetrahedral Fe^{2+} coordinations in the A′ column.

distance. The average Ca–O distance of 2.58 Å is shorter than the expected value of 2.61 Å from ionic radii, whereas the A-site Fe–O distances of 2.08 and 2.10 Å are longer than expected values of 2.01 and 2.02 Å for tetrahedral and square planar coordinations, repectively. This reveals lattice strain from ordering large Ca^{2+} and small Fe^{2+} cations in alternate A-site columns of the perovskite framework.

Magnetisation data for the $CaFeFeNbO_6$ sample are shown in Fig. 4. The susceptibility χ in Fig. 4a reveals paramagnetic behaviour, and the effective magnetic moment per $CaFeFeNbO_6$ unit (calculated as $\mu_{eff} = 2.83\sqrt{(\chi T)}$) at high temperatures (>250 K) is close to the theoretical spin-only value of 7.7 μ_B for high spin Fe^{2+} and Fe^{3+} cations, hence confirming the mixed Fe-valency in $CaFe^{2+}Fe^{3+}Nb^{5+}O_6$. However, the inverse susceptibility plot (shown in ESI,‡ Fig. S8) does not show a linear (Curie–Weiss) variation over the paramagnetic regime, most likely due to impurity contributions. A broad susceptibility peak is observed at 12 K with divergence of zero-field cooled (ZFC) and field-cooled (FC) susceptibilities. This peak shifts to low temperature as applied field increases (Fig. 4b), and to higher temperature with increasing frequency in ac measurements (Fig. 4c). These

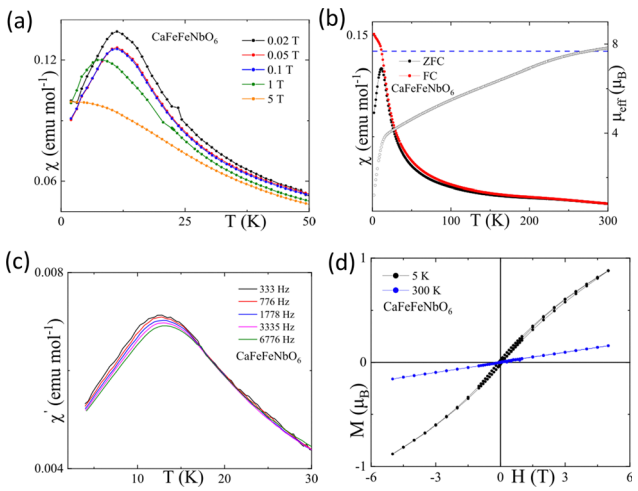

Fig. 4 Magnetic measurements for $CaFeFeNbO_6$. (a) ZFC and FC susceptibilities under a 0.1 T field, and the effective moment (calculated from FC susceptibilities) which approximates to the theoretical value of 7.68 μ_B (blue dashed line) near 300 K. (b) Low temperature ZFC susceptibility under varying fields. (c) Low temperature ac susceptibility at several frequencies. (d) Magnetisation-field loops at 5 and 300 K.

susceptibility variations, and also the slightly non-linear and hysteretic magnetisation-field loop at 5 K (Fig. 4d), are all characteristic of a spin-glass, and further analysis of the ac susceptibility peak shift is shown in ESI,‡ Fig. S9.

Comparison of variable temperature powder neutron patterns for the $CaFeFeNbO_6$ sample in Fig. 5 show two peaks that appear on cooling at long-d and so are most likely magnetic in origin. A prominent magnetic intensity appears on the peak at d = 4.59 Å from the $CaFeO_{3-x}$ impurity on cooling from 300 to 150 K. The magnetic transition is thus above that of stoichiometric $CaFeO_{3-x}$ (120 K)[29] but below that of the O-vacancy ordered brownmillerite $CaFeO_{2.5}$ (730 K),[30] consistent with the presence of O-vacancies in this impurity. A weak second peak at d = 4.93 Å arises between 150 and 2 K. This could be associated with the 12 K magnetic transition in $CaFeFeNbO_6$ but the peak does not index on the $P4_2/n$ cell or simple supercells. As spin order in previous studied $P4_2/n$ double double perovskites is usually ferrimagnetic and commensurate with the unit cell, and would give rise to strong magnetic diffraction peaks for high spin Fe^{2+} and Fe^{3+} cations, it is more likely that the d = 4.9 Å peak is due to spin ordering in an impurity phase.

The magnetisation results discussed above plus the lack of clear magnetic diffraction peaks show that $CaFeFeNbO_6$ is a spin-glass below freezing temperature $T_f \approx 12$ K. This can be attributed to the high degree of disorder between magnetic Fe^{3+} and non-magnetic Nb^{5+} cations over the B-sites. Spin glass ground states were also reported for $CaMnFeTaO_6$ which has substantial Fe/Ta disorder,[21] and in Sr_2FeNbO_6[27] and many other cation-disordered double perovskites. The substantial Fe/Nb disorder in $CaFeFeNbO_6$ also masks potentially interesting magnetic and conducting properties related to Fe^{2+}/Fe^{3+} charge transfer which could lead to ferromagnetic double exchange as found in magnetite.

Results for the $CaMFeNbO_6$ (M= Mn) analogue shown in ESI,‡ are very similar to those for M = Fe. $CaMnFeNbO_6$ adopts

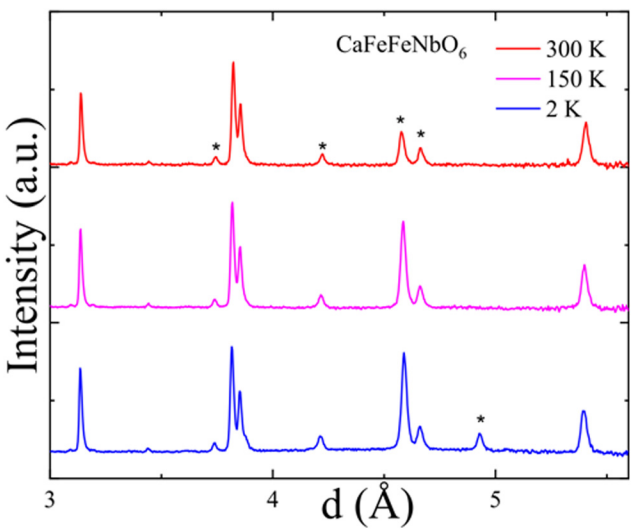

Fig. 5 Comparison of long-d powder neutron patterns for the $CaFeFeNbO_6$ sample at several temperatures with impurity peaks marked*.

the $P4_2/n$ double double perovskite structure with a substantial (29%) Fe/Nb disorder at the B-sites, and also has 16% substitution of Fe for Mn at the A' sites, so the phase has overall stoichiometry $CaMn_{0.84}Fe_{1.16}NbO_6$. $CaMnFeNbO_6$ shows paramagnetic behaviour at high temperatures and has a magnetic susceptibility peak at 27 K that shifts to higher temperature with increasing frequency in ac measurements. This and a lack of any magnetic diffraction peaks down to 2 K evidence a spin glass ground state.

$CaFeFeNbO_6$ is the first reported $AA'BB'O_6$ $P4_2/n$ double double perovskite based on A' = Fe. As many A/A' columnar-ordered perovskites are based on A' = Mn but few with other metals, it is useful to compare synthesis pressures for analogue pairs; $CaA'Ti_2O_6$, A' = Mn (7 GPa)[12] and Fe (14–15 GPa);[7] $CaA'FeReO_6$, A' = Mn (10 GPa)[18] and Cu (15.5 GPa);[24] and here $CaMFeNbO_6$; A' = Mn (10 GPa) and Fe (14 GPa). The extra synthesis pressures for other A' cations relative to Mn^{2+} are in the range 4–8 GPa implying that further analogues of known $AMnBB'O_6$ double double perovskites (synthesised at 10 GPa) may be accessible at pressure of 14 to 18 GPa for A' = Fe, Cu and other divalent cations of a similar size. It is also notable that $CaFeTi_2O_6$ was initially synthesised at 14–15 GPa, but crystals were subsequently grown at 12 GPa using water as a mineraliser, so pressures for growth of new double double perovskites may be lowered by a few GPa in the same way.

In conclusion, $CaFeFeNbO_6$ is the first reported example of a $P4_2/n$ $AA'BB'O_6$ double double perovskite based on A' = Fe. The synthesised samples are stoichiometric with Fe^{2+}/Fe^{3+} mixed valence, however, potentially interesting magnetic properties related to charge transfer are masked by antisite Fe/Nb disorder that leads to a spin glass ground state below a freezing transition at 12 K. The $CaMnFeNbO_6$ analogue also shows substantial cation disorder and spin glassy behaviour. Comparison of optimum synthesis pressures for the latter and other pairs of ordered materials based on different A-site transition metals, suggests that pressures of at least 14–18 GPa will be required to discover the expected plethora of double double perovskites based on cations smaller than Mn^{2+}.

We thank EPSRC for support, and STFC for provision of access to ISIS and ILL.

Conflicts of interest

There are no conflicts to declare.

References

1 G. King and P. M. Woodward, *J. Mater. Chem.*, 2010, **20**, 5785–5796; M. Shaikh, A. Fathima, M. J. Swamynadhan, H. Das and S. Ghosh, *Chem. Mater.*, 2021, **33**, 1594–1606; A. Ghosh, G. Palanichamy, D. P. Trujillo, M. Shaikh and S. Ghosh, *Chem. Mater*, 2022, **34**, 7563–7578.
2 M. T. Anderson, K. B. Greenwood, G. A. Taylor and K. R. Poeppelmeier, *Prog. Solid State Chem.*, 1993, **22**, 197–233.
3 C. J. Howard, B. J. Kennedy and P. M. Woodward, *Acta Crystallogr., Sect. B: Struct. Sci.*, 2003, **59**, 463–471.
4 S. Vasala and M. Karppinen, *Prog. Solid State Chem.*, 2015, **43**, 1–36.
5 K.-I. Kobayashi, T. Kimura, H. Sawada, K. Terakura and Y. Tokura, *Nature*, 1998, **395**, 677–680.
6 D. Serrate, J. De Teresa and M. Ibarra, *J. Phys.: Condens. Matter*, 2006, **19**, 023201.
7 K. Lienenweber and J. Parise, *J. Solid State Chem.*, 1995, **114**, 277–281.
8 G. Shimura, K. Niwa, Y. Shirako and M. Hasegawa, *Eur. J. Inorg. Chem.*, 2017, 835–839.
9 A. A. Belik, L. Zhang, R. Liu, D. D. Khalyavin, Y. Katsuya, M. Tanaka and K. Yamaura, *Inorg. Chem.*, 2019, **58**, 3492–3501.
10 R. Liu, D. D. Khalyavin, N. Tsunoda, Y. Kumagai, F. Oba, Y. Katsuya, M. Tanaka, K. Yamaura and A. A. Belik, *Inorg. Chem.*, 2019, **58**, 14830–14841.
11 R. Liu, R. Scatena, D. D. Khalyavin, R. D. Johnson, Y. Inaguma, M. Tanaka, Y. Matsushita, K. Yamaura and A. A. Belik, *Inorg. Chem.*, 2020, **59**, 9065–9076.
12 A. Aimi, D. Mori, K.-I. Hiraki, T. Takahashi, Y. J. Shan, Y. Shirako, J. Zhou and Y. Inaguma, *Chem. Mater.*, 2014, **26**, 2601–2608.
13 M. Fukuda, T. Nishikubo, Z. Pan, Y. Sakai, M.-H. Zhang, S. Kawaguchi, H. Yu, Y. Okimoto, S.-Y. Koshihara, M. Itoh, J. Rödel and M. Azuma, *Inorg. Chem.*, 2020, **59**, 11749–11756.
14 L. Zhang, Y. Matsushita, K. Yamaura and A. A. Belik, *Inorg. Chem.*, 2017, **56**, 5210–5218.
15 E. Solana-Madruga, Á. M. Arévalo-López, A. J. Dos Santos-García, E. Urones-Garrote, D. Ávila-Brande, R. Sáez-Puche and J. P. Attfield, *Angew. Chem., Int. Ed.*, 2016, **55**, 9340–9344.
16 E. Solana-Madruga, Á. M. Arévalo-López, A. J. Dos santos-García, C. Ritter, C. Cascales, R. Sáez-Puche and J. P. Attfield, *Phys. Rev. B*, 2018, **97**, 134408.
17 K. Ji, Y. Yuan, G. T. Moyo, C. Ritter and J. P. Attfield, *J. Solid State Chem.*, 2022, **313**, 123329.
18 G. M. McNally, Á. M. Arévalo-López, P. Kearins, F. Orlandi, P. Manuel and J. P. Attfield, *Chem. Mater.*, 2017, **29**, 8870–8874.
19 G. M. McNally, A. M. Arévalo-López, F. Guillou, P. Manuel and J. P. Attfield, *Phys. Rev. Mater.*, 2020, **4**, 064408.
20 E. Solana-Madruga, Y. Sun, Á. M. Arévalo-López and J. P. Attfield, *Chem. Commun.*, 2019, **55**, 2605–2608.
21 P. Kearins, E. Solana-Madruga, K. Ji, C. Ritter and J. P. Attfield, *J. Phys. Chem. C*, 2021, **125**, 9550–9555.
22 E. Solana-Madruga, P. S. Kearins, K. N. Alharbi, C. T. Lennon, C. Ritter and J. P. Attfield, *Phys. Rev. Mater.*, 2021, **5**, 054412.
23 K. Ji, K. N. Alharbi, E. Solana-Madruga, G. T. Moyo, C. Ritter and J. P. Attfield, *Angew. Chem., Int. Ed.*, 2021, **133**, 22422.
24 E. Solana-Madruga, P. S. Kearins, C. Ritter, A. M. Arévalo-López and J. P. Attfield, *Angew. Chem., Int. Ed.*, 2022, **61**, e202209497.
25 M. A. Patino, F. D. Romero, M. Goto, T. Saito, F. Orlandi, P. Manuel, A. Szabó, P. Kayser, K. H. Hong, K. N. Alharbi, J. P. Attfield and Y. Shimakawa, *Phys. Rev. Res.*, 2021, **3**, 043208.
26 L. C. Chapon, P. Manuel, P. G. Radaelli, C. Benson, L. Perrott, S. Ansell, N. J. Rhodes, D. Raspino, D. Duxbury, E. Spill and J. Norris, *Neutron News*, 2011, **22**, 22–25.
27 A. R. Chakhmouradian and R. H. Mitchell, *J. Solid State Chem.*, 1998, **138**, 272–277.
28 N. Kashima, K. Inoue, T. Wada and Y. Yamaguchi, *Appl. Phys. A: Mater. Sci. Process.*, 2002, **74**(Suppl.), S805–S807.
29 F. Kanamaru, H. Miyamoto, Y. Mimura, M. Koizumi, M. Shimada, S. Kume and S. Shin, *Mater. Res. Bull.*, 1978, **13**, 61–66.
30 M. Ceretti, A. Piovano, A. Cousson, T. Berthier, M. Meven, G. Agostini, J. Schefer, O. Hernandez, C. Lamberti and W. Paulus, *CrystEngComm*, 2012, **14**, 5771–5776.

